

Performance analysis of various rotor topologies of surface PM synchronous motor

Vasilija Sarac¹

Surface mounted permanent magnet synchronous motors can be found in several designs regarding configuration of magnets on the rotor. Finding the most optimal design in terms of the high efficiency and power factor, small cogging torque and material consumption along with good overloading capability could be a challenging task. This paper analyzes three different rotor designs of surface permanent magnet motors regarding their magnet shapes. All three motors have the same outer dimensions, output power, torque and the material properties. The comparison of all three models is performed and advantages and drawbacks of each model are pointed out. Four design variables are selected to be varied within prescribed limits for each motor model in order the best combination of number of conductors per slot, magnet thickness, the magnet length and shape to be found, which result with the highest efficiency, small cogging torque and good overloading capability of the motor. The impact of each varied parameter on motor efficiency and cogging torque is presented. All three optimized model are compared and the most optimal model in terms of the above-mentioned characteristics is analyzed by Finite Element Method (FEM) and with the Simulink. The model in Simulink allows motor transient characteristics to be obtained. The performed analysis is useful for determining the most optimal and cost-effective solution among presented three types of surface mounted permanent magnet motors in terms of the high efficiency and power factor, small cogging torque and material consumption.

Key words: surface mounted permanent magnet motor, efficiency, cogging torque, magnetic flux density distribution, transient characteristics

1 Introduction

Synchronous motors with permanent magnet has been known for their high efficiency and good power factor. There are numerous advantages that facilitates their usage in industrial processes or propulsion systems: high power density, no torque ripple when the motor is commutated, high efficiency at high speeds, easy maintenance and installation, capable of maintaining the full torque at low speeds, high reliability and efficient dissipation of heat. Among major drawbacks are the high initial costs and difficulties regarding starting up because it is not a self-starting motor. Depending on how magnets are attached to the rotor and the design of the rotor, permanent magnet synchronous motor can be classified into two types: surface permanent magnet synchronous motor (SPMSM) and interior permanent magnet synchronous motor (IPMSM). Also depending on the stator design, the permanent magnet motor can be with distributed or concentrated winding. There are various cases of synchronous motors designed, to keep the other parts almost unchanged compared to a corresponding asynchronous machine (eventually winding turns are changed). This kind of approach has spread in the last few years, with the aim of satisfying generic applications, precisely as substitution of the asynchronous motor. Besides the evident advantages in manufacturing costs, the use of equivalent parts in terms of overall dimensions, supports and external fixing points, has allowed adopting these motors with-

out modifying the remaining mechanics [1]. Whenever the permanent magnet synchronous motor design in question is, there are numerous design solutions often calculated by design assist systems that allow accurate calculation of motor characteristics that satisfy the predefined motor operating conditions [2]. Majority of these software use the methods for motor calculating based on equivalent motor circuits that account various motor losses such as core losses [2-4]. The constant need for energy efficient motors has determined the main research directions in permanent magnet synchronous motors *ie* influence of various construction parameters such as magnet material or combination of several types of magnet materials into hybrid magnets and their impact on motor efficiency and power factor [5]. Impact of the poles and slots combinations on motor noise and torque as one of the most important operating characteristics in the propulsion systems has been analyzed in [6-8]. The other authors searched for the reduction of noise at SPMSM by introducing the complex global air gap permeance per unit area in order to take into account the permeability of magnetic wedges, the height of pre-slot and the rotor shape [9]. Despite of all the benefits, especially in terms of the energy savings that come along with the use of permanent magnet synchronous motors instead of asynchronous motors there are still some difficulties in their usage that should be overcome. One of them is the cogging torque that originates from the interaction of rotor permanent magnets and stator slots and affects the motor control precision

¹ Faculty of Electrical Engineering, Goce Delcev University, Krste Misirkov 10-A, 2000 Stip, North Macedonia, vasilija.sarac@ugd.edu.mk

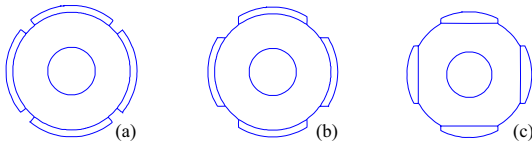


Fig. 1. Analyzed types of permanent magnet motors

especially in low speed applications. The rotors magnets tend to align with the stator in the position in which the air gap permeance is larger so when they are shifted from this position, they generate a torque know as cogging torque. Skewing of the stator slots can effectively eliminate the cogging torque in case when it is accurately analytically calculated [10]. Yet, this method demands complex production of the stator, which cannot be taken from the corresponding asynchronous motor, increased manufacturing costs and overall motor price. Therefore, this method for cogging torque reduction, although effective, cannot be easily implemented in practice. Other design parameters such as combinations of number of slots and poles and magnet arc affect the magnitude of the cogging torque at SPMSM. Therefore, the factor proportional to the slots number and the poles number and inversely proportional to their smallest common multiple has been introduced to indicate the goodness of the combination of number of slots and poles [11]. The magnet wedges with central separator from low permeability material effectively reduces the maximum cogging torque according to [12]. Another aspect of minimization of cogging torque is the magnet shaping [13-16]. Various optimization methods have been compared with respect to the design objective such as machine weight, magnets weight or efficiency in [17]. Optimization of motor performance and comparison of various rotor topologies of SPMSM has been presented in [18]. However, the optimized models have different outer dimensions suggesting that comparison is done for different machines. Reduction the production cost of permanent magnet motors for traction applications is presented in [19]. The optimization procedure is applied on axial flux modular structure with straight slots and concentrated windings.

In this paper, the optimization of SPMSM is presented based on parametric analysis, a software module in Ansys software that allows several design parameters of the electrical machine to be varied within prescribed limits, in order to calculate numerous combinations out of these varied parameters, which define the various motor models. The advantage of the parametric analysis is that all motor operating characteristics that are selected for optimization, *ie* the efficiency, cogging torque, magnet mass, can be calculated and analyzed simultaneously for each combination of varied parameters, providing the broader perspective of the analyzed design. As it will be presented later, there can be more than one solution for each motor type with maximum efficiency or the smallest cogging torque. By analyzing all possible solutions, the optimal model with relatively high efficiency, small cogging torque, and good magnetic characteristics in terms of safe

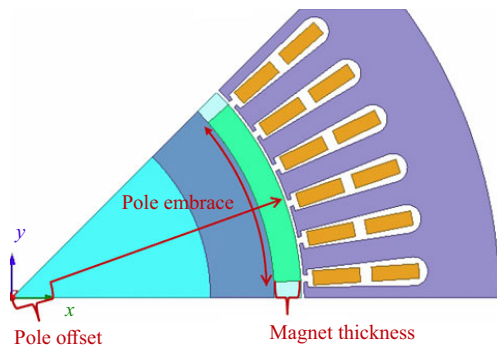
operation of the motor without the danger from demagnetization can be found. Firstly, three different rotor topologies for the same SPMSM are defined where the only differences are shape of the magnets and their dimensions.

For all of the three configurations the computer models are derived and the operating characteristics of each motor model are calculated. These motor models will be referred to as basic motor models of all three rotor topologies (BM1, BM2 and BM3). Parametric analysis is applied for all three models where the same set of varied parameters is used. From each of the three models (Fig. 1) 1376 new combinations (models) are obtained because of the parametric analysis. All obtained motor models are evaluated for several operating characteristics: efficiency, power factor, cogging torque, maximum power and permanent magnet material consumption. For each type of the motor, presented in Fig. 1, the most optimal solution is selected in terms of the efficiency, power factor, cogging torque and permanent magnet consumption. These optimized motor models will be referred to as OM1, OM2 and OM3 and they correspond to the optimized variant of models BM1, BM2 and BM3 respectively. Finally, from all three optimized models (OM1, OM2 and OM3), one most favorable model in terms of the efficiency, power factor, cogging torque and permanent magnet consumption is selected. The selected model is analyzed by Finite Element Method for magnetic flux density distribution. Over the years, Finite Element Method has proved to be a valuable tool in machine analysis in terms of calculating various electromagnet variables necessary for estimation of the goodness of the motor design [20, 21]. The last part of the analysis is obtaining the transient characteristics of current, speed and torque of the selected optimal model. Transient characteristics are integral part of motor analysis as they provide data of motor acceleration with various loads and the motor dynamic response [22, 23].

Searching for the most optimal motor design is always a challenging task and often it is a trade-off between the motor cost and performance. The presented analysis compares the various types of SPMSM and makes their additional optimization. Moreover, the impact of each varied parameter to the motor characteristics, subject to designers interest, can be individually analyzed and adequate conclusion can be derived that contribute to improvement of the machine design. Finally, finding the motor optimal design is a complex process where several operating characteristics of the motor should be taken into consideration in selecting the most optimal design, as it will be presented later. By employing the optimization per one parameter, *ie* efficiency or cogging torque, several models can be designed, with the highest efficiency but significantly deteriorated remaining parameters like the cogging torque or magnet mass. Therefore, the implemented approach of parametric analysis offers broader perspective of the designing process which facilitates the most optimal and cost-effective solution of the analyzed design.

Table 1. Main motor dimensions and winding parameters

| Dimensions/winding parameters | BM1&BM2 | BM3 |
|-------------------------------|---------|------|
| Stator outer diameter (mm) | 163 | 163 |
| Rotor outer diameter (mm) | 97 | 97 |
| Rotor outer diameter (mm) | 95.2 | 95.2 |
| Motor length (mm) | 105 | 105 |
| Number of stator slots | 36 | 36 |
| Winding layers | 2 | 2 |
| Nr. of parallel branches | 2 | 2 |
| Conductors per slot | 92 | 92 |
| Coil pitch | 7 | 7 |
| Magnet thickness (mm) | 3.4 | 8 |
| Pole embrace (mm) | 0.85 | 0.6 |
| Pole offset (mm) | 5 | 6 |

**Fig. 2.** Representation of geometry of permanent magnet parameters [26]

2 Parametric analysis and results

In this analysis the approach of modification of asynchronous squirrel cage motor (AM) into surface permanent magnet motor was adopted. The starting point is asynchronous squirrel cage motor, the product of company Rade Konar from Zagreb, H2AZ 155-4 of IE3 class of efficiency. The technical data concerning this motor can be found in [24]. Firstly, the computer model of the asynchronous motor in Ansys software was derived. More data about this model can be found in [25]. The second step was to derive three models of SMSPM according to the presented rotor topologies in Fig. 1.

Some constrains were adopted during the modeling process. The motor outer dimensions are the same for all three types of SMSPM and they remain unchanged, compared to AM. The same materials were used in SMSPMs as in the AM. The rotor dimensions remain also unmodified, only the squirrel cage winding was replaced by permanent magnets. Three models of SMSPM were derived according to rotor topologies presented in Fig.1 and they are referred to as basic models BM1, BM2 and BM3. The design constrain according to which the models were derived is that all models should have the same

output power of 2.2 kW. The samarium cobalt permanent magnets were used in all three models. The main dimensional data for all three models are presented in Tab. 1. The main differences between first two models and the third one, are dimensions concerning permanent magnets *ie* magnet thickness, pole embrace and pole offset, taking into account that all three models are modeled according to the generic designs of the rotors presented in Fig. 1. Therefore, although BM1 and BM2 have the same design parameters according to Tab. 1 the different rotor configuration *ie* magnets cutting will have impact on operating characteristics of the motors. The pole embrace represents the ratio of the pole arc to the pole pitch, pole offset is pole arc center offset from the rotor center while magnet thickness is the thickness of the magnets mounted on the rotor surface. They are presented in Fig. 2. Pole offset modification within certain ranges, *ie*, shaping the magnets, should improve the motor cogging torque therefore, it is adopted as one of the design parameters that should be optimized.

Table 2. Comparison of operating characteristics of BM1 to BM3

| | BM1 | BM2 | BM3 |
|---------------------------------|-------|-------|--------|
| Rated output power- P_2 (kW) | 2201 | 2201 | 2200 |
| Rated current - I_1 (A) | 3.62 | 3.58 | 3.65 |
| Rated torque - T_n (Nm) | 14 | 14 | 14 |
| Speed - n_n (rpm) | 1500 | 1500 | 1500 |
| Efficiency - η (%) | 91.75 | 91.89 | 91.78 |
| Power factor - $\cos \varphi$ | 0.99 | 0.99 | 0.98 |
| Maximum power - P_{max} (W) | 8278 | 8052 | 107481 |
| Cogging torque - T_{cog} (Nm) | 0.27 | 0.14 | 0.58 |
| Magnet mass m (kg) | 0.64 | 0.65 | 0.9 |

Table 3. Range of variation of optimization variables

| Variable | Range (BM1-BM2) | Step | Range (BM3) | Step |
|---------------------------------------|-----------------|------|-------------|------|
| No. of conductors per stator slot-CPS | 90 - 100 | 1 | 90 - 100 | 1 |
| Magnet thickness- MT (mm) | 3.2 - 3.6 | 0.1 | 8 - 10 | 1 |
| Pole offset OFS (mm) | 3 - 7 | 1 | 3 - 6 | 1 |
| Pole embrace EMB | 0.83 - 0.87 | 0.01 | 0.5 - 0.7 | 0.1 |

The three models BM1 to BM3 have different operating characteristics, obtained as output from the computer models, modeled in RMXprt, software module of Ansys. They are presented in Tab. 2. The obtained data in Tab. 1 are compared with the similar motor with the

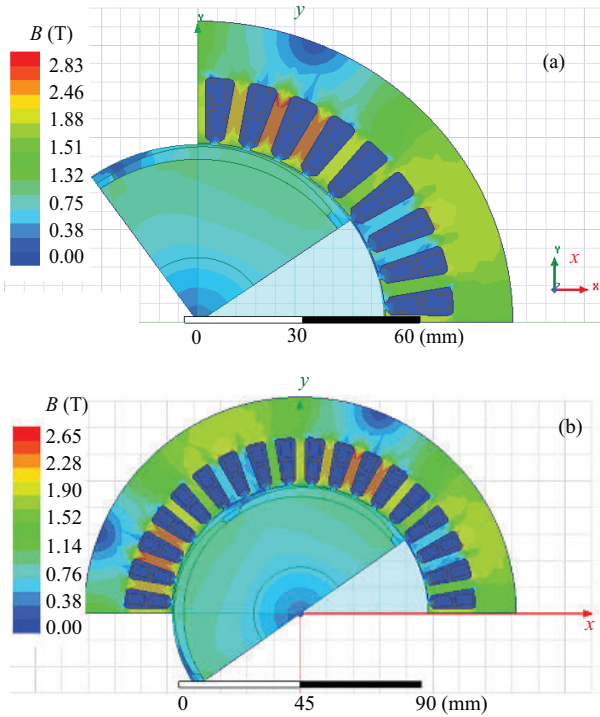


Fig. 4. Flux density distribution at motor cross-section at motor starting: (a) – OM1-3, (b) – OM2-10

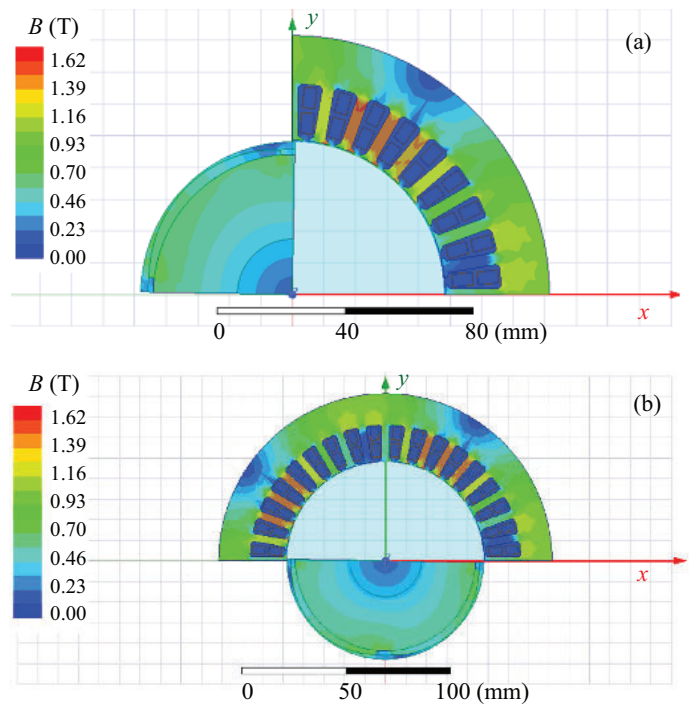


Fig. 5. Flux density distribution at motor cross-section-near synchronous speed: (a) – OM1-3, (b) – OM2-10

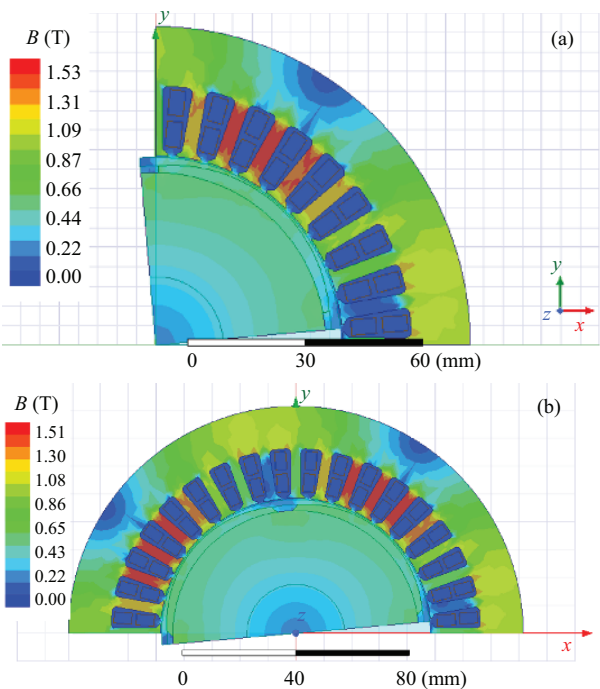


Fig. 6. Flux density distribution at motor cross-section at synchronous speed (a) – OM1-3, (b) – OM2-10

els the dimensions of all motors remain unchanged. The number of conductors in stator slot, magnet thickness, pole embrace and pole offset are selected for variation. Their ranges of variation, also the variation step, for all three models are presented in Tab. 3.

For the model BM1 and BM2, 1375 combinations of varied parameters exist, *ie* each of these combinations defines the new motor model. The criteria for selecting the optimized model is the high efficiency with improved *ie* considerably smaller cogging torque than the starting models BM1 and BM2. The criteria for choosing the highest efficiency for most favorable solution of the optimized model, leads to several solutions, each of them has the highest efficiency, but the other parameters of interest, like cogging torque or permanent magnet weight considerably differs from one model to another. Therefore, for BM1 exist twelve optimized models with the highest efficiency and similarly for model BM2 exist nine optimized model with the highest efficiency and one model, which has high efficiency, slightly lower than the highest value, but very small cogging torque. Therefore, it is also included in the selection of the best candidates for optimized model of BM2. From the optimized models of BM1, there is no other model, which has smaller cogging torque than the already selected twelve models, which have already satisfied the both criteria of the highest efficiency and the small cogging torque. The optimized models of BM1 and BM2 are presented in Tab. 4 and 5 respectively. For easier evaluation of all optimized models, the cogging torque and magnet weight are added in Tab. 4 and 5. These optimized models of BM1 will be referred to as OM1-1 to OM1-12 and for BM2 will be referred to as OM2-1 to OM2-10.

The model OM1-3 (Tab. 4) is chosen as the best candidate regarding the optimization of BM1. The criteria for choosing the OM1-3 is the smallest cogging torque considering that all optimized models in Tab. 4 have the

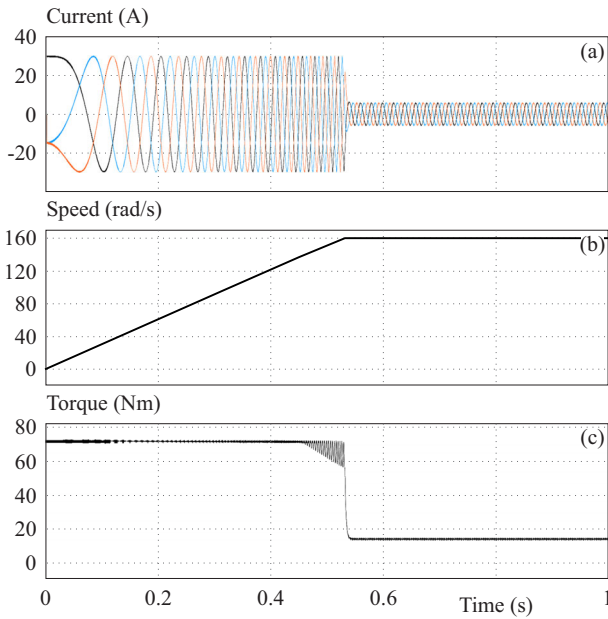


Fig. 7. Transient characteristics of current, speed and torque for model OM2-10

same efficiency, which is, actually the highest efficiency obtained from the parametric analysis of BM1. Model OM2-10 is selected as the best candidate from all optimized models in Tab. 5. The reason for selecting this model was that the efficiency is almost the same as in the other nine models but the cogging torque of this model is considerably smaller than at the other models. In Tab. 6 comparatively are presented the best candidates of optimized models of all three motors BM1, BM2 and BM3. The optimized model of BM3 is referred to as OM3 and it was selected among 396 combinations of varied parameters on the base of the highest efficiency as at all optimized models of BM3, 396 in total, the cogging torque is considerably bigger than in optimized models of BM1 and BM2.

According to the presented results in Tab. 6, it can be concluded that in terms of the efficiency and cogging torque the model OM2-10 could be the optimal solution. The cogging torque is considerably smaller than in the other two models and the efficiency is almost as high as in model OM1-3. As the difference in efficiency between model OM1-3 and OM2-10 is not so significant, the model OM2-10 is selected as the best candidate among all optimized motor models. OM2-10 is analyzed with FEM and modeled in Simulink for obtaining the transient characteristics. Model OM3 besides bigger cogging torque, has considerable bigger consumption of permanent magnet material so in comparison with the other two optimized models of SPMSM does not represent the cost effective solution. The efficiency, air-gap flux density and cogging torque of models BM2 and OM2-10, comparatively, are presented in Fig. 3. They should support the data presented in Tabs. 2 and 5.

3 Results from FEM analysis

Finite Element Method has been often used for verification of machine models *ie* for more exact calculation of magnetic flux density in machine cross-section. The method allows points of the magnetic core with high saturation to be detected and improved by modification of the design. The core saturation contributes to increased losses and motor heating. The FEM models have been created for optimized models OM1-3 and OM2-10, taking into consideration that these two models are selected as the best candidates regarding efficiency and the cogging torque among the three analyzed rotor topologies. The distribution of magnetic flux density is calculated for both models and for various operating regimes, *ie* starting, near the synchronous speed and at steady-state operation of the motor. For starting regime, the magnetic flux density for OM1-3 and OM2-10 is presented in Fig. 4 and for operation near synchronous speed in Fig. 5.

In Fig.6 is presented the distribution of magnetic flux density at synchronous speed for both models.

4 Results from Simulink analysis

The model OM2-10 is analyzed by Simulink in a closed-loop speed and current control. The motor is fed by a PWM inverter. The PWM inverter is built entirely with standard Simulink blocks. Its output goes through controlled voltage source blocks before being applied to the permanent magnet synchronous block's stator windings. The load torque applied to the machine's shaft is set to its nominal value 14 Nm [28].

Two control loops are used. The inner loop regulates the motor's stator currents. The outer loop controls the motor's speed [28]. The motor speed is set to 157.15 rad/s or 1500 rpm. The motor is loaded with 14 Nm load. As an output from the motor block, transient characteristics of current, speed and torque are obtained. They are presented in Fig. 7.

5 Discussion of results

Finding the most optimal and cost-effective design of the electrical motor is always a challenging task. In case of permanent magnet synchronous motor with surface mounted magnets, there are numerous variants of the magnets shapes and dimensions and the winding parameters. On the other hand, the designed motor should have satisfactory performance parameters: high efficiency, small cogging torque and consumption of permanent magnet material. By implementing parametric analysis, that allows variation of several parameters and simultaneous calculation of output results such as efficiency, cogging torque and permanent magnet weight the various motor models can be obtained and evaluated on the base of several performance parameters giving to the designer

Table 6. The best candidates of optimized models

| | OM1-3 | OM2-10 | OM3 |
|---|---------|--------|--------|
| CPS | 90 | 91 | 90 |
| MT (mm) | 3.5 | 3.6 | 8 |
| OFS (mm) | 7 | 6 | 6 |
| EMB (mm) | 0.87 | 0.87 | 0.6 |
| I_1 (A) | 3.57 | 3.56 | 3.55 |
| Frictional and windage losses- P_{fw} (W) | 44 | 44 | 44 |
| Iron core losses- P_{Fe} (W) | 40.8 | 41.3 | 40.2 |
| Copper losses- P_{Cu} (W) | 93.97 | 94.3 | 93.2 |
| Input power P_1 (W) | 2379.75 | 2380.5 | 2377.4 |
| Outout power- P_2 (W) | 2201 | 2201 | 2200 |
| η (%) | 92.49 | 92.45 | 92.54 |
| $\cos \varphi$ | 0.99 | 0.99 | 0.99 |
| M_{cog} (Nm) | 0.116 | 0.0652 | 0.58 |
| m_m (kg) | 0.63 | 0.68 | 0.9 |

a broader perspective of the analyzed problem. Moreover, the analysis can be implemented on different rotors configuration with surface permanent magnets such as with parallel magnets, trapezoidal magnets and broad-loaf magnets. The analysis was carried out on comparable basis: all models have same output power, dimensions and built-in materials. According to the data presented in Tab. 4 and by evaluating all performance parameters, efficiency, cogging torque and magnet mass, the model OM1-3 is selected as the best optimized model of first type of the motor with parallel magnets. From the data presented in Tab. 5 it is evident that if solely efficiency is selected as parameter according to which the most optimal model is searched, it leads to several possible motor models which are not necessarily the most optimal or cost effective solutions. On the base of presented parameters, efficiency, cogging torque and magnets mass the model OM2-10 was selected as the best-optimized model of the second type of the motor with trapezoidal magnets. Following the same analogy, the best candidate among all models of third type of the motor with broad-loaf permanent magnets is selected and presented in Tab. 6 as model OM3. In Tab. 6 is presented a comparison between all selected optimized models of all three types of the motor with surface magnets. All three selected optimized models have nearly the same efficiency. The difference is in cogging torque and permanent magnets weight. The models OM1-3 and OM2-10 outperform the model OM3 with respect to the cogging torque and magnets weight. Therefore, model OM3 is excluded from further analysis as it cannot be the most optimal and cost-effective solution. The both selected candidates as the best-optimized models OM1-3 and OM2-10 are analyzed with FEM for magnetic flux density distribution. According to the results presented in Figs. 4, 5 and 6, the model OM2-10 shows

satisfactory distribution of magnetic flux density in all three operating regimes: starting, before synchronization and at operation with synchronous speed and no demagnetization of the magnets should occur. The model OM1-3 is subject to partial demagnetization of the magnets in all three operating regimes. The model OM1-3 has thinner magnets, compared to model OM2-10 (3.5 mm compared to 3.6 mm respectively) and the pole offset is bigger at OM1-3 than in OM2-10, which results in thinner edges of the magnets, subject of demagnetization. In all three types of rotors the same type of magnet is used SmCo28 with residual flux density of 1.07 T and coercive force of 820 kA/m. In order to provide fair comparison between different rotor topologies, the first rotor model was also analyzed with the same data as the second rotor topology (OM2-10), *ie* CPS = 91, MT = 3.6 mm, EMB = 0.87, OFS = 6 mm. It was found out that in this case, for the motor with the parallel-sided magnets, the efficiency is 92.3%, cogging torque is 0.14 Nm and magnet mass is 0.67 kg or the performance parameters are worse than at motor with trapezoidal magnets. In general, the motor with parallel magnets shows somewhat smaller efficiency and bigger cogging torque in comparison to the rotor topology with trapezoidal magnets. Considering above mentioned analysis and results, the model OM2-10 shows the most satisfactory performances from all analyzed models and it could be considered as the best candidate, considering efficiency and cogging torque, of all three analyzed rotor topologies. The model OM2-10 is modeled in Simulink for obtaining transient characteristics. Transient characteristics, presented in Fig. 7 are modeled for set rated speed as a reference speed and for acceleration with the rated load. After the acceleration has finished the motor reaches the nominal speed, current and torque. Motor successfully synchronizes with the network and maintains the synchronous speed. The impact of each varied parameter (CPS, MT, EMB, OFS) on efficiency and cogging torque is analyzed for the model OM2-10 and they are presented in Fig. 8 and 9 respectively. In Fig. 8(a) is presented the impact of CPS on cogging torque for the model OM2-10, when all the other parameters are like in model OM2-10 (MT = 3.6 mm, EMB = 0.87, OFS = 6 mm). Similarly on Fig. 8(b) is presented the impact of EMB on cogging torque for the model OM2-10, and the other parameters are like in model OM2-10 (MT = 3.6 mm, OFS = 6 mm, CPS = 91). The same analogy is implemented in Fig. 8(c) and (d) for the impact of MT and OFS on the cogging torque.

The number of conductors per slot or CPS has no impact on motor cogging torque. Pole embrace and pole offset have the most significant impact on the cogging torque. The increase of pole offset reduces the cogging torque but the magnets can become too thin, which increases the risk of demagnetization. The cogging torque increases with magnet thickness but as mentioned, too thin magnets increase the risk of demagnetization so the optimal magnets thickness should be provided with the design of the machine. Furthermore, the motor current

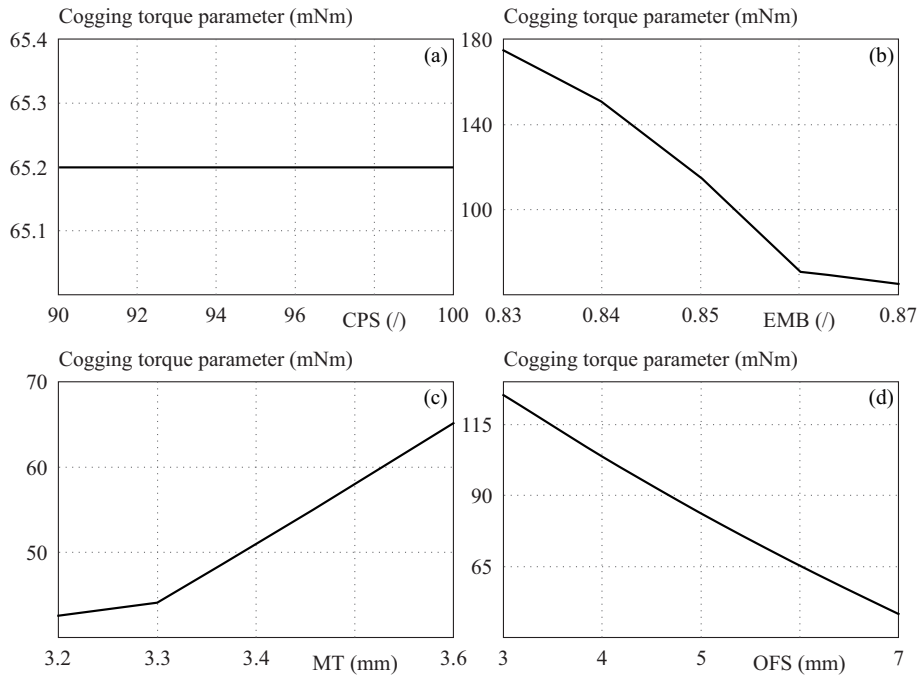


Fig. 8. Impact of varied parameter on cogging torque-model OM2-10

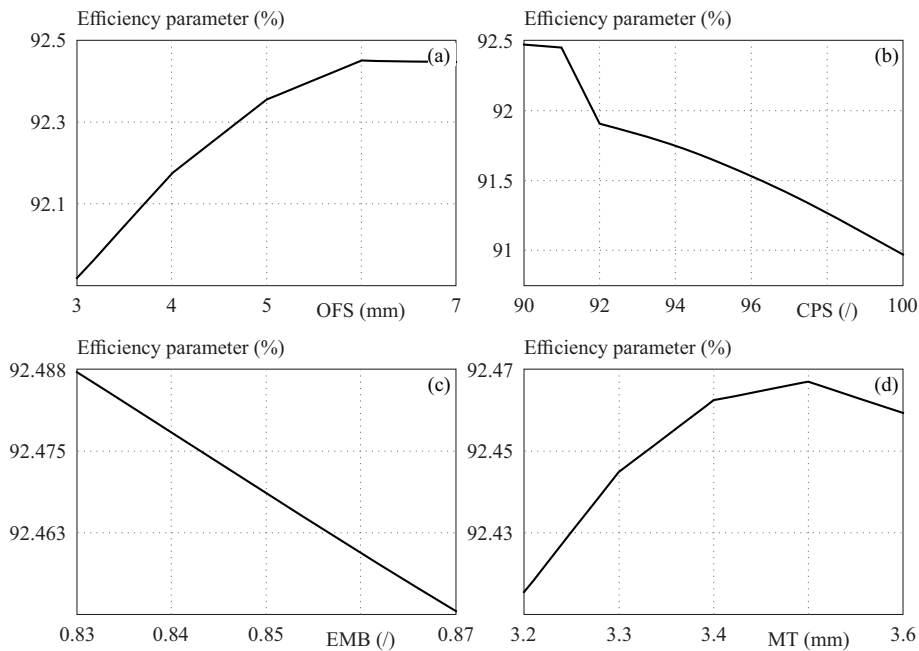


Fig. 9. Impact of varied parameters on efficiency-model OM2-10

increases when the magnets are thinner and efficiency decreases as well. The increase of pole embrace decreases the cogging torque but increases the magnet weight and cost of material.

The impact of four varied parameter on motor efficiency is presented in Fig. 9. The impact each parameter on efficiency is analyzed while the other three parameters have values as presented in Tab. 5 for model OM2-10.

The most significant impact on efficiency has CPS. The increase of CPS decreases the efficiency due to increase of resistance and copper losses. The pole embrace

has insignificant impact on efficiency and with the increase of pole embrace the efficiency insignificantly decreases. Similar finding can be found in [29]. Variation of magnet thickness from 3.2 mm to 3.6 mm increases the efficiency due to decreased current and the copper losses. Yet, the magnet thickness is not so critical for the efficiency and the thickness can be reduced slightly without significantly reducing the efficiency. The increase of pole offset decreases the induced phase voltage and current so the copper losses are reduced and efficiency is increased, Fig. 10. According to this, the increase of pole offset has

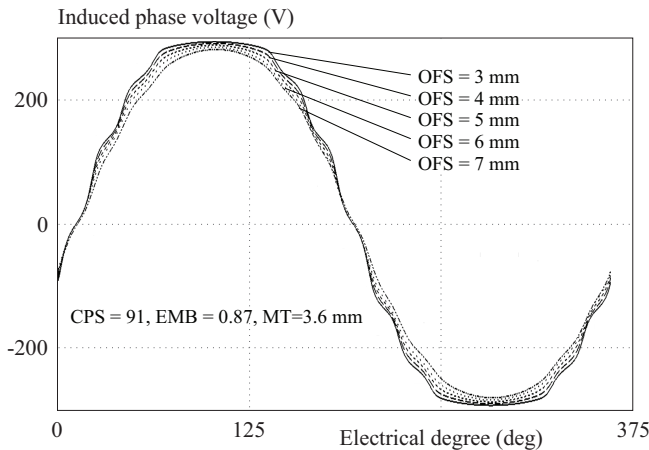


Fig. 10. Induced phase voltage for various pole offsets

also impact on shape of the induced voltage, which is becoming more sinusoidal with the increase of the pole offset.

The presented models are theoretical ones. The efficiency of the prototype as well as other relevant operating parameters is highly dependent on manufacturer tolerances and the quality of in-built materials. The presented analysis and models is for power supply of 50 Hz. The operation of the motor with various frequencies *ie.*, operating speeds is subject to further research and analysis. However, the presented analysis can contribute to viewing the motor design as complex multi-parameter dependent process where the optimal solution can be found by evaluating several operating characteristics correlated to various motor design parameters.

6 Conclusion

The paper analyzes synchronous permanent magnet motors with surface magnets on the rotor, which can be found in three most common rotor topologies: with parallel magnets, trapezoidal magnets and broad-loaf magnets. Finding the most optimal rotor topology with respect to the motor efficiency, cogging torque and magnet mass could be a challenging task. There are various motor designs in each of these three rotor topologies, which engage several design parameters. We will name some of them such as magnet shape, coverage of rotor with magnet poles, magnet thickness, and number of conductors per slot. They can vary from one design to another resulting in different motor models with various operating characteristics like efficiency, power factor, cogging torque and magnet mass. Finding the most optimal model in each of the three topologies with high efficiency, small cogging torque and magnets weight requires extensive calculations, which in this paper are done by parametric analysis. Parametric analysis calculates various motor models on the base of combinations of selected parameters (magnet thickness, pole offset, pole embrace

and number of conductors per slot) which are varied in predefined boundaries. For the rotor with parallel and trapezoidal magnets 1396 combinations of varied parameters, exist. For the rotor with broad-loaf magnets exist 386 combinations of varied parameters. Out of these numerous combinations, one design for each rotor type is selected which has high efficiency, small cogging torque and permanent magnets mass. However, not only the efficiency was taken into consideration as criteria for selection of the most optimal design. If only one operating characteristic is selected as optimization criteria, not always the most optimal design is obtained or selected. For the rotor with parallel magnets, twelve designs exist with the same efficiency (which is found to be the biggest for the analyzed problem) but all of them have different cogging torque and magnet mass. The parametric analysis calculates simultaneously several operating characteristics therefore provide the broader perspective of the analyzed optimized model. By comparing the best candidates from parametric analysis of all three types of rotor configuration, the rotor with trapezoidal magnets is found to be the best model with high efficiency, the smallest cogging torque and relatively small permanent magnet mass. This model is verified by FEM and shows satisfactory distribution of flux density at various operating speeds. The motor dynamics is analyzed by Simulink. The analysis of dynamics shows that motor accelerates up to the synchronous speed and maintains it, at rated load, when it is operated by the inverter.

The analysis in this paper is focused on finding the most optimal motor design among three different rotor topologies of surface permanent magnet synchronous motor concerning efficiency, cogging torque and magnet mass, which was successfully realized with the aid of presented parametric analysis.

The presented analysis is for power supply of 50 Hz. The impact of frequency variation to motor operating characteristics at various speeds and in so-call field weakening region is subject to further research. The presented models are theoretical. Therefore, the final motor performance can vary in dependence of manufacturing tolerances and quality of in-built material of the prototype.

REFERENCES

- [1] K. Yamano, S. Morimoto, M. Sanada, and Y. Inoue, "Design of Surface Permanent Magnet Synchronous Motor Using Design Assist System for PMSM", *IEEJ Journal of Industry Application*, vol. 6, no. 6. pp. 409-415, DOI: 10.1541/ieejia.6.409, 2017.
- [2] X. Ba, Z. Gong, Y. Guo, C. Zhang, and J. Zhu, "Development of Equivalent Circuit Models of Permanent Magnet Synchronous Motors Considering Core Loss", *Energies*, vol. 15, no. 6, <https://doi.org/10.3390/en15061995>, 2022.
- [3] E. K. Beser, "Electrical equivalent circuit for modeling permanent magnet synchronous motors", *Journal of Electrical Engineering*, vol. 72, no. 3. pp. 176-183, <https://doi.org/10.2478/jee-2021-0024>, 2021.
- [4] S. Mabrak, S. Chakroune, and D. Khodija, "Analytical Model of Slotted Surface Mounted Permanent Magnet Synchronous Motors with Non-magnetic Rotor Core", *Modeling, Measurement and*

- Control*, A, vol. 92, no. 2-4. pp. 60-66, <https://doi.org/10.18280/mmc.a.922-404>, 2019.
- [5] B. Slusarek, D. Kapelski, L. Antal, P. Zalas, and M. Gwodziewicz, "Synchronous Motor with Hybrid Permanent Magnets on the Rotor", *Sensors*, vol. 14, <https://doi.org/10.3390%2Fs140712425>, 2014.
- [6] F. Pop-Piglesan, F. Jurca, C. Oprea, and C. Martis, "Permanent magnet synchronous machine design for low-noise drive systems", *Proceedings of ISMA2014 including USD2014*, pp. 1387-1400, 2014.
- [7] G. Verez, G. Barakat, Y. Amara, and G. Hoblos, "Impact of Pole and Slot Combination on Vibrations and Noise of Electromagnetics Origins in Permanent Magnet Synchronous Motors", *IEEE Transactions on Magnetics*, vol. 51, no. 3, <https://doi.org/10.1109/TMAG.2014.2354019>, 2015.
- [8] Y. Liu, Zi-Qiang Zhu, C. Gan, S. Brockway, and C. Hilton, "Comparison of optimal slot/pole number combinations of fractional slot permanent magnet synchronous machines having similar slot and pole numbers", *The Journal of Engineering*, no. 17. pp. 4585-4589, <https://doi.org/10.1049/joe.2018.8202>, 2019.
- [9] M. Fakam, M. Hecquet, V. Lanfranchi, and A. Randria, "Design and magnetic noise reduction of the Surface Permanent Magnet Synchronous Machine using complex air gap permeance", *IEEE Transactions on Magnetics*, vol. 51, no. 4, 2015, pp. 8103809, DOI: 10.1109/TMAG., 2360315, 2014.
- [10] J. Si, S. Zhao, L. Zhang, R. Cao, and W. Cao, "The Characteristics Analysis and Cogging Torque Optimization of a Surface-Interior Permanent Magnet Synchronous Motor", *Chinese Journal of Electrical Engineering*, vol. 4, no. 4. pp. 41-47, <https://doi.org/10.23919/CJEE.2018.8606788>, 2018.
- [11] Z. Q. Zhu, "Influence of Design Parameters on Cogging Torque in Permanent Magnet Machines", *IEEE Transactions on Energy Conversion*, vol. 15, no. 4. pp. 407-412, <https://doi.org/10.1109/60.900501>, 2000.
- [12] I. M. Garcia-Garcia, Á. J. Romero, J. H. Ciudad, and S. M. Arroyo, "Cogging Torque Reduction Based on a New Pre-Slot Technique for a Small Wind Generator", *Energies*, vol. 11. 3219, <https://doi.org/10.3390/en11113219>, 2018.
- [13] N. Chen, S. L. Ho, and W. N. Fu, "Optimization of Permanent Magnet Surface Shapes of Electric Motors for Minimization of Cogging Torque Using FEM", *IEEE Transactions on Magnetics*, vol. 46 no. 6. pp. 2478-2481, <http://dx.doi.org/10.1109/TMAG.2010.2044764>, 2010.
- [14] F. Sculler, "Magnet Shape Optimization to Reduce Pulsating Torque for a Five-Phase Permanent-Magnet Low-Speed Machine", *IEEE Transactions on Magnetics*, vol. 50, no. 4. pp. 1-9, <https://doi.org/10.1109/TMAG.2013.2287855>, 2014.
- [15] C.-S. Lee, K.-S. Cha, J.-C. Park, and M.-S. Lim, "Tolerance-Insensitive Design of Magnet Shape for a Surface Permanent Magnet Synchronous Motor", *Energies*, vol. 13, 1311, <https://doi.org/10.3390/en13061311>, 2020.
- [16] M. Aydin, O. Ocak, and Y. Demir, "Influence of varying magnet pole-arcs and step-skew on permanent magnet AC synchronous motor performance", *Turkish Journal of Electrical Engineering & Computer Science*, vol. 28. pp. 3304-3318, <https://doi.org/10.3906/elk-2003-179>, 2020.
- [17] Y. L. Karnavas, I.D. Chasiotis, and E.L. Peponakis, "Permanent Magnet Synchronous Motor Design Using Grey Wolf Optimizer Algorithm", *International Journal of Electrical and Computer Engineering*, vol. 6, no. 3. pp. 1353-1362, <http://doi.org/10.11591/ijece.v6i3.pp1353-1362>, 2016.
- [18] W. Purwanto, Risfendra, D. Fernandez, D. S. Putra, and T. Sugiarto, "Design and Comparison of five Topologies Rotor Permanent Magnet Synchronous Motor for High-Speed Spindle Applications", *International Journal of GEOMATE*, vol. 13, no. 40. pp. 148-154, <https://doi.org/10.21660/2017.40.02765>, 2017.
- [19] R. Neji, S. Tounski, and F. Sellami, "Contribution to the definition of a permanent magnet motor with reduced production cost for the electrical vehicle propulsion", *European Transactions on Electrical Power*, vol. 16. pp. 437-460, <http://dx.doi.org/10.1002/etep.95>, 2006.
- [20] G. Pellegrino, A. Vagati, B. Boazzo, and P. Gugliemi, "Comparison of Induction and PM Synchronous motor drives for EV application including design examples", *IEEE Transactions on Industry Application*, vol. 48, no. 6. pp. 2322-2332, <http://dx.doi.org/10.1109/TIA.2012.2227092>, 2012.
- [21] B.-H. Lee, H.-I. Park, and J.-W. Jung, "Design of Surface-Mounted Permanent Magnet synchronous Motor Considering Axial Leakage Flux by using 2-Dimensional Finite Element Analysis", *Journal of Electrical Engineering & Technology*, vol. 13, no. 6. pp. 2284-2291, <https://doi.org/10.5370/JEET.2018.13.6.2284>, 2018.
- [22] M. Korkosz and G. Podskarbi, "Laboratory Test of Surface Mounted Permanent Magnet Brushless Motor", *Technical Transactions Electrical Engineering*, 3-E. pp. 185-195, DOI: 10.4467/2353737XCT.16.276.6075, 2016.
- [23] L. Antal and P. Zalas, "Soft and synchronous starting of low-power SMPMSM motor", *Przeegl Elektrotechniczny*, vol. 89, nr. 2b/2013. pp. 173-176, 2012.
- [24] "Koncar-Mes", Available online, <https://koncar-mes.hr/wp-content/uploads/2020/08/Electric-motors.pdf> (accessed on 01 February 2023).
- [25] V. Sarac, "Design Optimization of Induction Motor for Efficiency and Reliability Improvement", *30th International Conference on Organization and Technology of Maintenance OTO 2021, Lecture Notes in Networks and Systems*, vol. 369 pp. 35-49, Springer, Cham, https://doi.org/10.1007/978-3-030-92851-3_3, 2021.
- [26] Ansys Inc. *Maxwell 2D Users Guide 2010*, Ansys Inc.: Canonsburg, PA, USA, 2020.
- [27] "OME Motors", Available online, <https://www.omemotors.es/media/catalogo/es/OMPM%20CATALOGUE.pdf> (Accessed on 01. February 2023).
- [28] Mathworks, Available online, <https://www.mathworks.com/help/sps/ug/permanent-magnet-synchronous-machine.html> (Accessed on 03. February 2023).
- [29] C. Ocak, I. Tarimer, A. Dalcali, and D. Uygun, "Investigation Effects of Narrowing Rotor Pole Embrace to Efficiency and Cogging Torque at PM BLDC Motor", *TEM Journal*, vol. 5, no. 1. pp. 25-31, <https://dx.doi.org/10.18421/TEM51-04>, 2016.

Received 24 January 2023

Vasilija Sarac, full professor of the Faculty of Electrical Engineering at Goce Delcev University, Stip, Republic of North Macedonia. Her main research interests include design, simulation and optimization methods of electrical machines and power converters.